

# A Relaxation Solution for Transonic Flow over Three-Dimensional Jet-Flapped Wings

W.D. Murphy\* and N.D. Malmuth†  
Rockwell International, Thousand Oaks, Calif.

An algorithm has been developed which treats transonic flow over jet-flapped wings of general planform within a small disturbance framework. The numerical method represents a generalization of the relaxation solutions developed by Bailey and Ballhaus for unblown wings and the authors' previous work for two-dimensional jet-flapped airfoils, and it incorporates a new far field which accounts for the vorticity on the jet. Supercritical results presented for a variety of blown planforms indicate repeal of the Kutta condition, as in two dimensions, appreciable spanwise load carryover for partial span blowing, and reduction in lift augmentation due to sweepback. Comparison of lift coefficients with experimental values shows good agreement for various planforms.

## Introduction

**P**ROPULSIVE lift systems such as the jet flap have been proposed as a means of developing high, buffet-free lift coefficients at transonic speeds. Although these devices have been studied extensively at low Mach numbers, our understanding of the associated physical processes in supercritical flow is limited. Toward the enhancement of this body of knowledge and interpretation of existing experimental data, relaxation methods recently have been applied by Ives and Melnik<sup>1</sup> and Malmuth and Murphy<sup>2</sup> to treat two-dimensional airfoils in the transonic regime. The Ives-Melnik analysis was restricted to zero angle of attack. For the Malmuth-Murphy solution, validations were obtained with experiments, and the nature of the lift augmentation and the asymptotic far field were explored. Because typical configurations employ low aspect ratio wings with fairly general planforms, three-dimensional effects can alter significantly the benefits predicted by two-dimensional models. These effects are complex and are not accessible to simple empirical modifications of the two-dimensional solutions such as strip and sweepback theory. However, modern relaxation methods applied within a three-dimensional small-disturbance framework now makes feasible the treatment of these configurations.

In this paper, the two-dimensional algorithm in Ref. 2 will be extended to handle jet-flapped three-dimensional wings of arbitrary planform and spanwise distributions of blowing. For this purpose, the far field expressions developed by the authors for two-dimensional jet-flapped airfoils and those obtained by Klunker<sup>3</sup> for unblown wings will be generalized to treat blown finite span wings. A byproduct of the far field developments is the asymptotic jet development and downwash in the Trefftz plane, which will be obtained in the limit of small blowing coefficient,  $C_\mu$ .

The numerical method will be described in some detail and

represents a generalization of the schemes of Murman and Cole,<sup>4</sup> Krupp and Murman,<sup>5</sup> Bailey and Ballhaus,<sup>6,7</sup> and those of the authors in Ref. 2. Special procedures will be indicated for dealing with the vortex sheet as a free boundary in this problem. The algorithm will be applied in this paper to evaluation of the flow over some trapezoidal planforms. Results will be presented for pressures and lift coefficients for these wings. The latter will be compared with experiments. Spanwise load distributions also will be evaluated against linearized lifting surface theory and studied as a function of flap angle and spanwise extent of blowing.

## Formulation

The transonic small disturbance formulation for pure lifting wings using scaled coordinates is described in Ref. 6. Referring to Fig. 1, these coordinates are defined in terms of the analogous dimensional (barred) coordinates and flow parameters as follows

$$x = \bar{x}/c$$

$$y = \bar{y}/b$$

$$z = \delta^{1/3} M_\infty^{2/3} (\gamma + 1)^{1/3} \bar{z}/c$$

Here,  $c$  is the root chord,  $b$  is the wing semispan,  $\delta$  is the root thickness ratio,  $M_\infty$  is the freestream Mach number, and  $\gamma$  is the ratio of the specific heats. Assuming small flow deflections and a freestream Mach number near unity, the approximate equation for a scaled version  $\Phi$  of the dimensional perturbation potential  $\phi$  is

$$(K_1 - \Phi_x) \Phi_{xx} + K_2 \Phi_{yy} + \Phi_{zz} = 0 \quad (1)$$

where

$$K_1 = (1 - M_\infty^2) / [\delta M_\infty^2 (\gamma + 1)]^{2/3}$$

$$K_2 = c^2 / b^2 [\delta M_\infty^2 (\gamma + 1)]^{2/3}$$

$$\Phi = M_\infty^{2/3} (\gamma + 1)^{1/3} \bar{\phi} / U_\infty c \delta^{1/3}$$

where  $U_\infty$  is the freestream velocity. In accordance with the small disturbance approximation and the planar nature of the configuration, the wing surface boundary conditions are transferred to the plane  $x_{LE} \leq x \leq x_{TE}$ ,  $-1 \leq y \leq 1$ , and  $z = 0$ .

If the wing upper and lower surfaces are given, respectively, by  $\bar{z}_u/c = \delta f_u(\bar{x}/c, \bar{y}/b)$  and  $\bar{z}_l/c = \delta f_l(\bar{x}/c, \bar{y}/b)$ , then the

Presented as Paper 76-98 at the AIAA 14th Aerospace Sciences Meeting, Washington, D.C., Jan. 26-28, 1976; submitted Feb. 5, 1976; revision received July 12, 1976. We would like to acknowledge informative discussions with F.R. Bailey and W.F. Ballhaus of NASA Ames Research Center and thank them for copies of their pure lifting three-dimensional program. The authors also express their appreciation to E.R. Cohen for his helpful comments on certain portions of the analysis.

Index categories: Subsonic and Transonic Flow; Jets, Wakes, and Viscid-Inviscid Flow Interactions.

\*Member of Technical Staff, Mathematical Sciences Group, Science Center.

†Program Manager, Fluid Dynamics, Science Center. Associate Fellow AIAA.

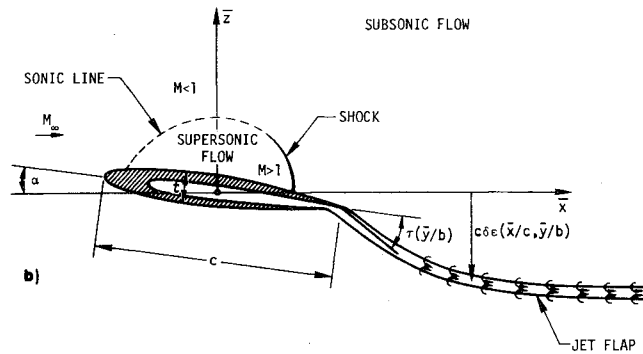
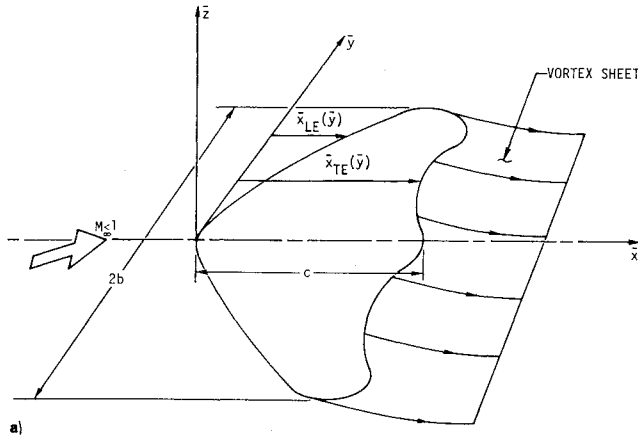


Fig. 1 a) Three-dimensional jet-flapped wing geometry. b) Flowfield configuration for plane  $y=0$  where  $\delta$  = root thickness ratio,  $\alpha$  = angle of attack,  $M_\infty = U_\infty / \alpha_\infty$  = Mach number, and  $c$  = root chord.

boundary conditions there are

$$\left( \frac{\partial \Phi}{\partial z} \right)_{u,l} (x, y, 0 \pm) = \left( \frac{\partial f}{\partial x} \right)_{u,l} (x, y) - \alpha / \delta \quad (2)$$

for  $x_{LE} \leq x \leq x_{TE}$ , where  $\alpha$  is the angle of attack of the wing.

Addition of a jet flap requires the inclusion of two new boundary conditions, namely,

$$[\Phi_x] \equiv \Phi_x(x, y, 0+) - \Phi_x(x, y, 0-) = C_\mu(y) \epsilon_{xx}(x, y) \quad (3'')$$

and

$$\Phi_z(x, y, 0 \pm) = \epsilon_x(x, y), \quad x > x_{TE}, \quad -1 \leq y \leq 1 \quad (4)$$

where  $c\delta\epsilon(\bar{x}/c, \bar{y}/b)$  represents the position of the jet sheet in physical coordinates and  $C_\mu(y)$  is a transonically scaled blowing parameter given by

$$C_\mu(y) \equiv (\gamma + 1)^{1/2} M_\infty^{4/3} \delta^{2/3} C_j(y) / 2$$

where, if  $q$  is the freestream dynamic pressure,  $J(y)$  is the momentum flux per unit span, then  $C_j(y)$ , the blowing coefficient, is given by  $C_j(y) = J(y)/qc$ . The parameter  $C_\mu$  has been regarded as an arbitrary and discontinuous function of  $y$ , allowing consideration of fairly general partial-span blowing schemes.

Consistent with the transfer of the wing boundary conditions, it should be noted that the jet boundary conditions (3'') and (4) also have been linearized to the plane  $z=0$ .

The initial condition on the jet slope is given by

$$\epsilon_x(x_{TE}, y) = -[\alpha + \tau(y)] / \delta, \quad -1 \leq y \leq 1 \quad (5)$$

where  $\tau(y)$  is the jet deflection angle as a function of  $y$ .

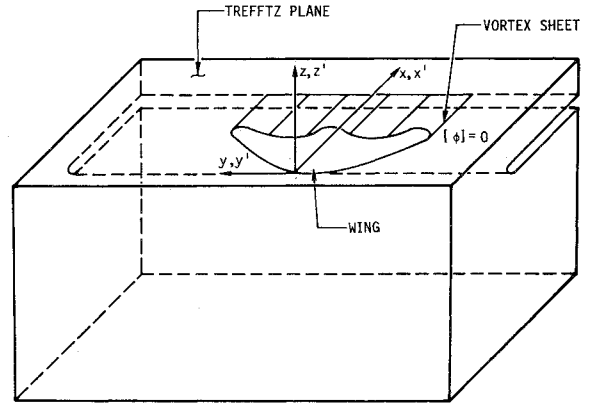


Fig. 2 Region for application of Green's theorem.

Equation (3'') now may be simplified by analytically integrating it in the  $x$  direction from  $x_{TE}$  to  $x$ . The result is

$$[\Phi] = [\Phi]_{x=x_{TE}} + C_\mu(y) \{ \epsilon_x(x, y) + [\alpha + \tau(y)] / \delta \} \quad (3)$$

$$x > x_{TE}, \quad -1 \leq y \leq 1$$

### Far Field

In accord with the procedures in Refs. 2-7, a subsonic far field may be obtained by application of Green's Theorem to the cut three-dimensional region shown in Fig. 2 to give the following integrodifferential equation

$$\phi(P) = \frac{\gamma + 1}{2K} \iiint_{-\infty}^{\infty} F(Q, P) \frac{\partial u^2}{\partial X'} dV_Q + \int_{-B}^B dY' \int_{x_{LE}}^{\infty} [\phi] \frac{\partial F}{\partial Z'} dX' - \int_{-B}^B dY' \int_{x_{LE}}^{x_{TE}} F(Q, P) \left[ \frac{\partial \phi}{\partial Z'} \right] dX' \quad (6')$$

where  $u = \phi_x$ . In (6'),  $P(X, Y, Z)$  and  $Q(X', Y', Z')$ , respectively, signify the field and source points in a coordinate system for which  $\phi(X, Y, Z) = (\gamma + 1)^{-1/2} \Phi(x, y, z)$ , and

$$X = \bar{x}/c$$

$$Y = \sqrt{K_1/K_2} y$$

$$Z = \sqrt{K_1} z$$

$K = (1 - M_\infty^2) / M_\infty^{4/3} \delta^{2/3}$ , and  $\phi$  is the scaled perturbation potential defined in Ref. 2. The brackets in (6') signify jumps in quantities across the plane  $z=0$ , and  $B = \sqrt{K_1/K_2}$ . In the  $(X, Y, Z)$  frame, (1) becomes a Poisson equation having nonlinear source term with the unit source fundamental solution,  $F(P, Q)$ , defined by

$$F(P, Q) = -1/4\pi\rho(P, Q) = F(Q, P)$$

where

$$\rho^2 \equiv (X - X')^2 + (Y - Y')^2 + (Z - Z')^2$$

and

$$\Delta F(P, Q) = \delta(P, Q)$$

The first and third terms in (6') are nonlinear volumetric and linear surface source distributions, respectively and are explicitly, (but not implicitly) the same as in the unblown case. The second integral is a doublet distribution associated with vorticity on the wing and its jet and differs from the unblown expressions in the portion of the inner integral taken along the vortex sheet  $x_{TE} \leq x \leq \infty$ . On this interval, the quantity  $[\phi]$

varies according to (3), rather than remaining constant as in the unblown case. By methods similar to those applied in Refs. 2 and 3, the dominant term can be shown to be the second integral. This integral, which will be denoted as  $\phi_{\text{lift}}$ , can be expressed as

$$\phi_{\text{lift}} = \frac{Z}{4\pi} \int_{-B}^B \rho_T^{-2} dY' \left\{ \int_{X_{LE}}^{X_{TE}} [u] \left( 1 + \frac{X-X'}{\rho_l} \right) dX' + C_\mu [\epsilon_X(\infty, Y') - \epsilon_X(X_{TE}, Y') + I] \right\}$$

where

$$I \equiv \int_{X_{TE}}^{\infty} \frac{(X-X')}{\rho_l} \frac{\partial^2 \epsilon}{\partial X'^2} dX'$$

$$\rho_l^2 \equiv (X-X')^2 + \rho_T^2, \rho_T^2 \equiv (Y-Y')^2 + Z^2$$

and

$$u = \partial \phi / \partial X$$

The integral  $I$  can be evaluated asymptotically by a procedure involving the subtraction and addition of the asymptotic form of the kernel function multiplying  $\partial^2 \epsilon / \partial X'^2$  in the integrand. The integral formed by grouping the difference between the exact and asymptotic kernel can be estimated to be a higher-order quantity than that involving the asymptotic kernel in the far field. Thus, to dominant order in the variables of (1),

$$\phi_{\text{lift}} \doteq \frac{1}{4\pi} \frac{z}{\bar{y}^2 + z^2} (1 + x/R) S + O(R^{-2}) \quad \text{as } R \rightarrow \infty \quad (6)$$

where  $R = [x^2 + K_l(\bar{y}^2 + z^2)]^{1/2}$ ,  $\bar{y} = y/\sqrt{K_2}$ , the local circulation,  $\Gamma(y)$ , is given by

$$\Gamma(y) = [\Phi(x_{TE}, y, 0) \equiv \Phi(x_{TE}, y, 0+) - \Phi(x_{TE}, y, 0-)]$$

and

$$S = \int_{-1/\sqrt{K_2}}^{1/\sqrt{K_2}} \{ \Gamma(y') + C_\mu(y') [\epsilon_X(\infty, y') - \epsilon_X(l, y')] \} dy'$$

Equation (6) is nonuniformly valid with respect to the intersection of the vortex sheet and the Trefftz plane,  $x = \infty$ ,  $y^2 < K_2^{-1}$ ,  $z = 0$ . For  $C_\mu \rightarrow 0$ , the behavior of the jet slope,  $\epsilon_x$  in the Trefftz plane can be obtained from a successive approximation solution of the appropriate modification of (6). This gives

$$2\pi\epsilon_X(X, Y) = \int_{-B}^B \frac{\Gamma'(u) du}{Y-u} + C_\mu \left\{ \int_{-B}^B \frac{du}{Y-u} \int_{-B}^B \frac{\Gamma'(u') du'}{u-u'} + A \ln \left| \frac{B+Y}{B-Y} \right| + \int_{-B}^B \frac{T(u) du}{Y-u} \right\} + O(X^{-2}, C_\mu^2)$$

$$\text{as } C_\mu \rightarrow 0, X \rightarrow \infty$$

where  $A = \alpha/\delta$ ,  $T(u) \equiv \tau(u)/\delta$ , and the Cauchy principle values are to be taken in the integrals. This asymptotic jet development can be used to establish the internal consistency of the approximations used in obtaining (6) and the calculation of wing-tail interference. It is interesting to note that the Trefftz plane downwash is nonvanishing, whereas for two-dimensional jet-flapped airfoils, it tends to zero as  $x \rightarrow \infty$ .

In contrast to the unblown or pure lifting wing, the second term in the integrand in Eq. (6') represents a contribution to the overall forces arising from "bound" vorticity in the wake. Analogous to the two-dimensional case, the potential at

points distant from the wing thus can be computed by lifting line theory. Whereas, in two dimensions, the vorticity is invariant along the infinite span, the finite aspect ratio wing sheds trailing vorticity, and the far field for the potential corresponds to a subsonically scaled version of the incompressible Biot-Savart expressions provided that the far field is subsonic. As in the two- and three-dimensional unblown cases, the nonlinear coupling of the spanwise loading and the near field must be determined from the numerical solution. This complication contrasts with the usual singular perturbation solution for an incompressible lifting line, discussed in Ref. 8, where the local circulation is obtained by matching inner and outer solutions.

For purposes of this analysis it was deemed advantageous to treat the transition from (6') to the appropriate representation on the vortex sheet in the Trefftz plane by a generalization of the numerical approach given in Refs. 6 and 7. The cross flow boundary value problem then involves the solution of

$$K_2 \Phi_{yy} + \Phi_{zz} = 0, \quad x > x_{TE} \quad (7)$$

with boundary conditions obtained from the asymptotic jet development given by

$$\Phi(x, y, 0 \pm) = 0, \quad x > x_{TE}, \quad |y| > l \quad (8a)$$

$$\Phi(x, y, 0 \pm) = \pm \{ \Gamma(y) + C_\mu(y) [\epsilon_X(\infty, y) - \epsilon_X(x_{TE}, y)] \} / 2$$

for  $x > x_{TE}, |y| \leq l$  (8b)

It should be noted that if  $C_\mu(y) = 0$ , then Eqs. (1-8) specialize to the appropriate forms in Ref. 6. This fact has allowed the algorithm of this paper to be designed to include the unblown code of Ref. 6 as a special case.

### Nonrectangular Wing Transformation

In Bailey and Ballhaus,<sup>7</sup> a description of the mapping of a swept and tapered wing into a rectangle is discussed. They define  $\xi = (x - x_{LE}) / (x_{TE} - x_{LE})$ ,  $\eta = y$ ,  $\zeta = z$ , where  $x_{LE}$  and  $x_{TE}$  are the  $x$ -coordinates of the leading and trailing edges, respectively. Under this transformation, Eqs. (1-5) become

$$[K_l \xi_x \Phi_\xi - (\xi_x \Phi_\xi)^2 / 2 + \xi_y K_2 (\xi_y \Phi_\xi + \Phi_\eta) / \xi_x]_\xi$$

$$[K_2 (\xi_y \Phi_\xi + \Phi_\eta) / \xi_x]_\eta + (\Phi_\zeta / \xi_x)_\zeta = 0 \quad (1')$$

$$\partial \Phi_{u,i}(\xi, \eta, 0 \pm) / \partial \zeta = \xi_x \partial f_{u,i}(\xi, \eta) / \partial \xi - \alpha / \delta$$

for  $0 \leq \xi \leq 1, -1 \leq \eta \leq 1$  (2')

$$[\Phi] = [\Phi]_{\xi=1} + C_\mu(\eta) \{ \xi_x \epsilon_\xi(\xi, \eta) + [\alpha + \tau(\eta)] / \delta \}$$

for  $\xi > 1, -1 \leq \eta \leq 1$  (3')

$$\Phi_\zeta(\xi, \eta, 0 \pm) = \xi_x \epsilon_\xi(\xi, \eta), \quad \xi > 1, -1 \leq \eta \leq 1 \quad (4')$$

$$\epsilon_\xi(l, \eta) = -[\alpha + \tau(\eta)] / \xi_x \delta, \quad -1 \leq \eta \leq 1 \quad (5')$$

### Numerical Procedure

The discretization of the partial differential equation (1') for parabolic, elliptic, hyperbolic, and shock-point operators is given in Ref. 7. We shall concentrate on how the new equations (3'-5') are handled. As in the two-dimensional case investigated by Malmuth and Murphy,<sup>2</sup> the jet stream  $\epsilon(\xi, \eta)$  is a free boundary, which is located during the iterative procedure. Using superscripts and the variable  $r$  to denote the iteration counter, we initially set

$$\epsilon_\xi^{(0)}(\xi, \eta) = \begin{cases} -[\alpha + \tau(\eta)] / \xi_x \delta, & \xi = 1 \\ \epsilon_\xi(l, \eta) (1 + 1/\xi^2) / 2, & \xi > 1 \end{cases}$$

This initialization is motivated by the asymptotic jet development given earlier. As the relaxation cycle sweeps from upstream to downstream, the values of  $[\Phi]_{\xi=1}$  are obtained in the usual way by extrapolation of the solution vector to the plane  $\zeta=0$  along the line  $\xi=1$ .

Equation (3') now is inserted into the discretization of the operator  $\Phi_{\xi\xi}$  at the plane above  $\zeta=0$  by replacing  $\Phi_{i,j,k-1}$  with

$$\Phi_{i,j,k-1} + [\Phi]_{\xi=1}^{(r)} + C_\mu(\eta_j) \{ \xi_x \epsilon_\xi^{(r)}(\xi_i, \eta_j) + [\alpha + \tau(\eta_j)] / \delta \}$$

and at the plane below  $\zeta=0$  by replacing  $\Phi_{i,j,k+1}$  with

$$\Phi_{i,j,k+1} - [\Phi]_{\xi=1}^{(r)} - C_\mu(\eta_j) \{ \xi_x \epsilon_\xi^{(r)}(\xi_i, \eta_j) + [\alpha + \tau(\eta_j)] / \delta \}$$

These expressions reduce to those of Bailey and Ballhaus<sup>7</sup> when  $C_\mu(\eta) \equiv 0$ . However, it should be noted that this approach assumes that  $\Phi_{\xi\xi}$  can be continued analytically across the vortex sheet. This is certainly true for the pure lifting case, since  $[\Phi_\xi] = [\Phi_{\xi\xi}] = [\Phi_{\eta\eta}] = [\Phi_{\xi\eta}] = 0$ . For the jet-flap, Eq. (3'') implies that  $[\Phi_{\xi\xi}] \neq 0$ . On the other hand,  $\epsilon_\xi$  and  $\epsilon_{\xi\xi}$  usually decay very rapidly especially for small  $C_\mu$ , and the condition  $[\Phi_{\xi\xi}] = 0$  is approximately valid everywhere on  $[1, \infty]$ , except in the immediate neighborhood of  $\xi=1$ . An alternate and more correct approach using averaging operators in the vicinity of the vortex sheet is discussed in Malmuth and Murphy<sup>2</sup> and the next section. The present method simplifies the programming enormously because there is now no need to have mesh points on the plane  $\zeta=0$ .

After the relaxation sweep is completed, updated values of the jet slope are obtained using condition (4') and numerical differentiations of  $\Phi_\xi(\xi, \eta, 0 \pm)$ , that is,

$$\epsilon_\xi^{(r+1)}(\xi_i, \eta_j) = (\Phi_{i,j,k}^{(r)} - \Phi_{i,j,k-1}^{(r)}) / \xi_x(\eta_j) (\zeta_k - \zeta_{k-1}) \quad (9)$$

Unfortunately, condition (9) cannot be imposed in the vicinity of the jet exit,  $\xi=1$ , because the singularity there leads to instabilities in the numerical procedure. In order to prevent such numerical difficulties, the "trick" is slightly to relax condition (4') for the first two mesh points to the right of the jet exit and to use Lagrange interpolation to calculate

$$\epsilon_\xi^{(r+1)}(\xi_{\text{jet}2}, \eta_j)$$

and

$$\epsilon_\xi^{(r+1)}(\xi_{\text{jet}3}, \eta_j)$$

using the initial condition (see Eq. 5')

$$\epsilon_\xi^{(r+1)}(\xi_{\text{jet}1}, \eta_j) \equiv \epsilon_\xi(I, \eta_j)$$

and the values

$$\epsilon_\xi^{(r+1)}(\xi_{\text{jet}4}, \eta_j), \quad \epsilon_\xi^{(r+1)}(\xi_{\text{jet}5}, \eta_j), \quad \epsilon_\xi^{(r+1)}(\xi_{\text{jet}6}, \eta_j)$$

and

$$\epsilon_\xi^{(r+1)}(\epsilon_{\text{jet}7}, \eta_j)$$

obtained from Eq. (9). Here  $\xi_{\text{jet}1}, \xi_{\text{jet}2}, \xi_{\text{jet}3}, \dots$  denote  $\xi$  points passing through the jet. This approach leads to remarkably smooth, rapid, monotone convergence of the maximum jet slope residual between successive iterations.

As in Ref. 2, line relaxation is employed to speed convergence. There, it was necessary to use three different choices for the relaxation parameter,  $\omega$ . When large values of  $\omega$  were used in the jet region, the iterative procedure diverged. This was due to instabilities created by the jet slopes changing each

iteration. For our present work, a much improved relaxation technique which is mainly an extension of that developed by Bailey and Ballhaus is applied. Associated with each point is a relaxation number that is prescribed by using over-relaxation for all elliptic points and under-relaxation for all other potential points in the field. In addition, the first point above and below the vortex sheet in the  $\zeta$  direction uses the under-relaxation value even if it may otherwise be an elliptic point. Now, line relaxation is employed using a vector of relaxation numbers for each line instead of a single relaxation parameter.

As discussed in Ref. 2, it is essential that each grid network have many points in the vicinity of the trailing edge of the wing in order to alleviate the problem of the change in the circulation lagging behind the maximum residual, a difficulty encountered by Ives and Melnik. Although this phenomenon sometimes occurs in our three-dimensional program, the lag is never by "orders of magnitude". In a typical example, when the maximum residual was  $10^{-5}$ , the maximum value of  $|\Gamma^{(r+1)}(\eta_j) - \Gamma^{(r)}(\eta_j)|$  was  $2 \times 10^{-5}$ .

The result of all these improvements is that the three-dimensional jet-flap program requires the same amount of computer execution time on the CDC 7600 as the pure lifting three-dimensional program, and pure lifting results can be obtained with no loss in accuracy as a special case of the jet-flap program by setting  $C_\mu(\eta) \equiv 0$ .

Once the maximum potential, circulation, and jet slope residuals have converged to say  $10^{-5}$ , the position of the jet stream  $\epsilon(\xi, \eta)$  may be obtained by numerically integrating  $\epsilon_\xi(\xi, \eta)$  with respect to  $\xi$ .

## Results and Discussion

For the following results, the fully conservative relaxation (FCR) method of Murman<sup>9</sup> is used with the lift and pressure coefficients defined as

$$C_L = \left( \frac{2\delta^{3/2} c}{\bar{c}(\gamma+1)^{1/2} M_\infty^{1/2}} \right) \int_0^I \left\{ \Gamma(\eta) + C_\mu(\eta) \xi_x(\eta) [\epsilon_\xi(\infty, \eta) - \epsilon_\xi(I, \eta)] \right\} d\eta$$

and

$$C_p(\xi, \eta, 0 \pm) = -[2\delta^{3/2} / (\gamma+1)^{1/2} M_\infty^{3/2} c(\eta)] \Phi_\xi(\xi, \eta, 0 \pm)$$

where  $c$  is the mean chord and  $c(\eta)$  is the local chord at the span station  $\eta$ . The point  $\infty$  is taken to be the largest  $\xi$  mesh point which is usually between 5 and 10, i.e., from 5 to 10 root chord lengths away from the leading edge of the wing. In addition, the reader will observe that the scaling on  $C_j(\eta)$  in this paper differs from that in Ref. 2 by a factor of  $(\gamma+1)^{1/2}/2$ , which is due to the difference between the definitions of the dimensionless variables in the two papers. In what follows, the earlier scaling is retained since it leads to better agreement with experimental lift data.

In Fig. 3, calculated chordwise loadings at  $M_\infty = 0.65$  and 0.85 are shown for a jet-flapped rectangular wing tested by Poisson-Quinton and Jousserandot.<sup>10</sup> The aspect ratio  $AR = 3$ ,  $\tau = 90^\circ$ ,  $\alpha = 0^\circ$ , and  $C_j = 0.02$  for this full span blown configuration. At  $M_\infty = 0.65$  subcritical conditions exist, and the wing appears highly two dimensional except in a small neighborhood of the tip, in spite of the relatively low value of  $AR$ . The repeal of the Kutta condition due to the blowing is also quite evident in this and the other cases to be discussed. For  $M_\infty = 0.85$ , a shock is evident near the trailing edge, and the three-dimensional effects become considerably more pronounced. The shock becomes attenuated progressively further outboard and the augmentation decreases with the spanwise loading as the tip is approached. To obtain these results, a fine grid ( $68 \times 35 \times 36$ ) was employed giving the lift coefficients indicated in the third column of the table.

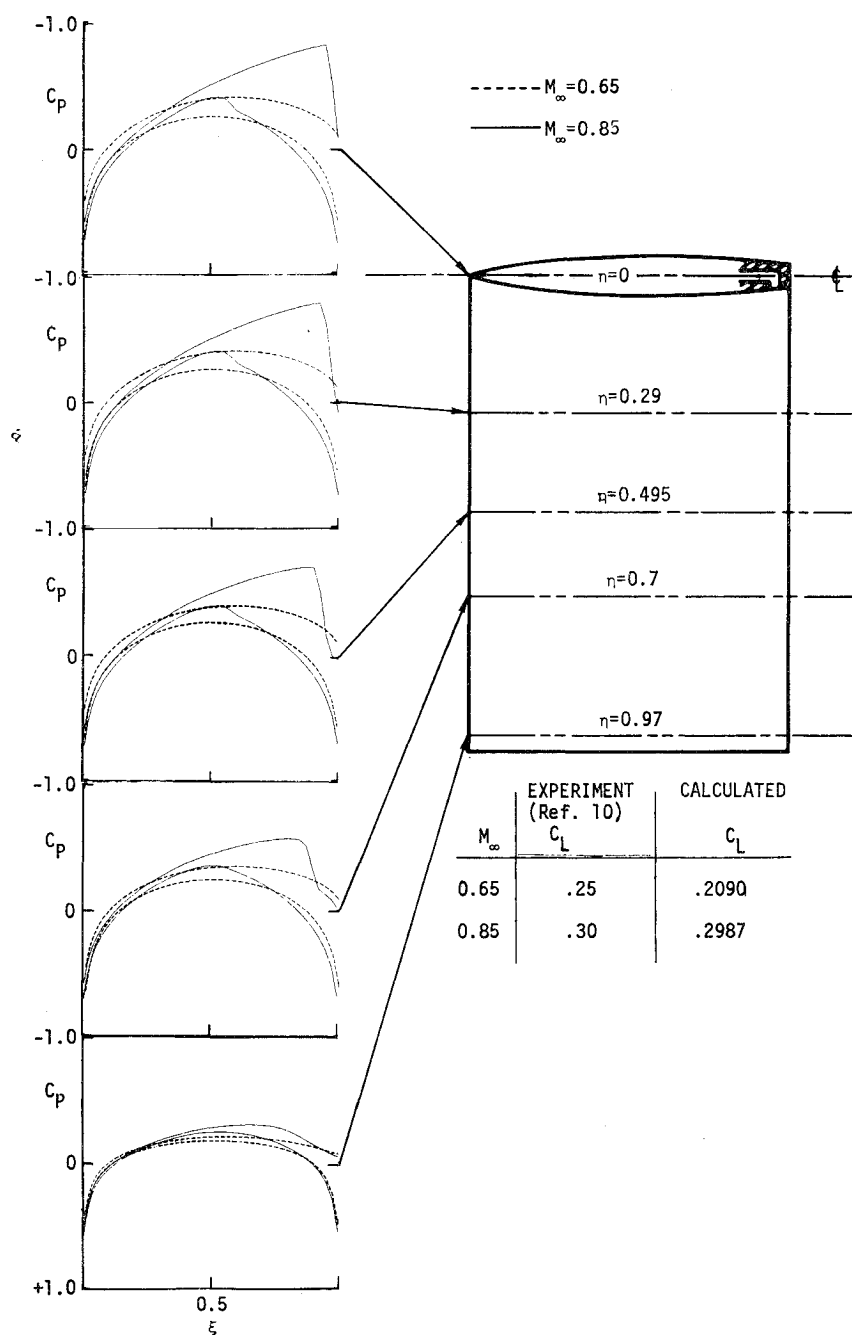


Fig. 3 Chordwise pressures on a jet-flapped rectangular wing,  $AR=3$ , for  $M_\infty=0.65$  and  $0.85$ ,  $\alpha=0^\circ$ ,  $\tau=90^\circ$ ,  $C_j=0.02$ , full span blowing.

The effect of sweepback on the foregoing results is depicted in Fig. 4, where the previous configuration is sheared downstream at a sweep angle of  $45^\circ$ . Chordwise pressures presented for  $M_\infty=0.85$  indicate considerable diffusion of streamwise gradients as the tip is approached. Moreover, the sweep reduces the effective normal Mach number, causing a return to subcritical-type chordwise pressure distributions. To prevent instabilities associated with the large sweepback, the grid was changed to  $(70 \times 36 \times 36)$  leading to a computed  $C_L$  of 0.2112. This results compares quite favorably to an experimental value of 0.19 obtained by Poisson-Quinton and Lepage<sup>11</sup> and suggests a supercritical reduction in augmentation due to sweepback. A similar trend was obtained at incompressible speeds by Malavard.<sup>12</sup>

Lift coefficients for a tapered wing considered without blowing in Ref. 7 are provided in Fig. 5 for full and inboard half-span blowing. These results were computed for the trapezoidal wing of Fig. 7 having a leading edge sweep,  $\Lambda=30^\circ$ ,  $AR=3.86$ , a taper ratio  $\lambda=0.538$  and an ONERA M6 symmetric section. The calculations were performed at  $M_\infty=0.84$ ,  $C_j=0.03$ , and  $\alpha=3^\circ$  on a crude  $(38 \times 20 \times 24)$  grid.

Accordingly, these results should be regarded as qualitative and approximate. As a frame of reference, the coarse grid value of  $C_L$  was computed to be 0.374 for  $\tau=30^\circ$  as compared to a fine  $(68 \times 35 \times 36)$  grid value of 0.424. The calculations suggest the persistence of a linear variation of  $C_L$  with  $\tau$  despite the supercriticality of the flow. Associated spanwise loadings are shown in Fig. 6. The anticipated enhancement in augmentation with increase of  $\tau$  is indicated in these distributions. Half span loadings also shown in this figure reveal appreciable carryover from blown to unblown sections of the wing. Presumably, the effect is associated with modified vortical induction from the blown region and mathematically may be due to the ellipticity of the spanwise flow. These results are in accord with experimental findings of Yoshihara and his co-workers.<sup>13</sup> Corresponding results obtained from a vortex lattice implementation of linearized lifting surface theory<sup>‡</sup> also are shown in Fig. 6. Strong qualitative similarity between both sets of variations is evident

‡Results were provided by W.C. Clever and E. Bonner.

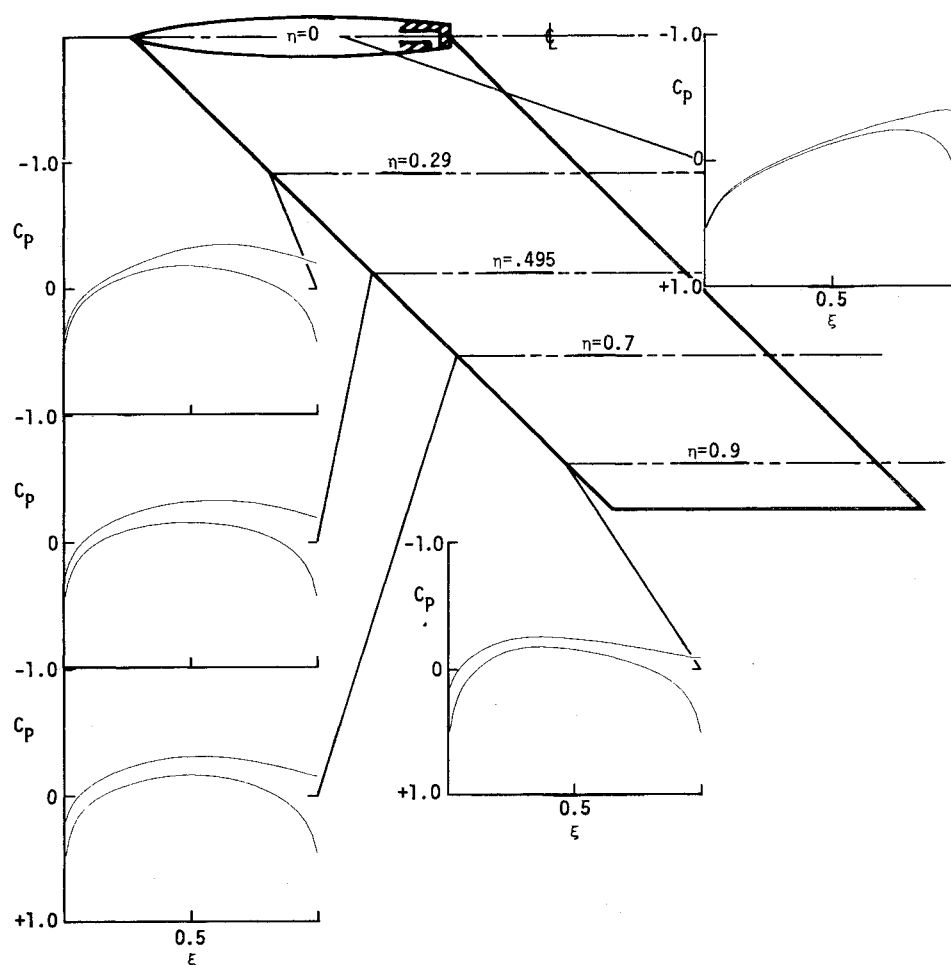


Fig. 4 Chordwise pressures on a swept, jet-flapped untapered wing.  $\Lambda = 45^\circ$ ,  $AR = 3$ ,  $M_\infty = 0.85$ ,  $\alpha = 0^\circ$ ,  $\tau = 90^\circ$ ,  $C_j = 0.02$ , full span blowing.

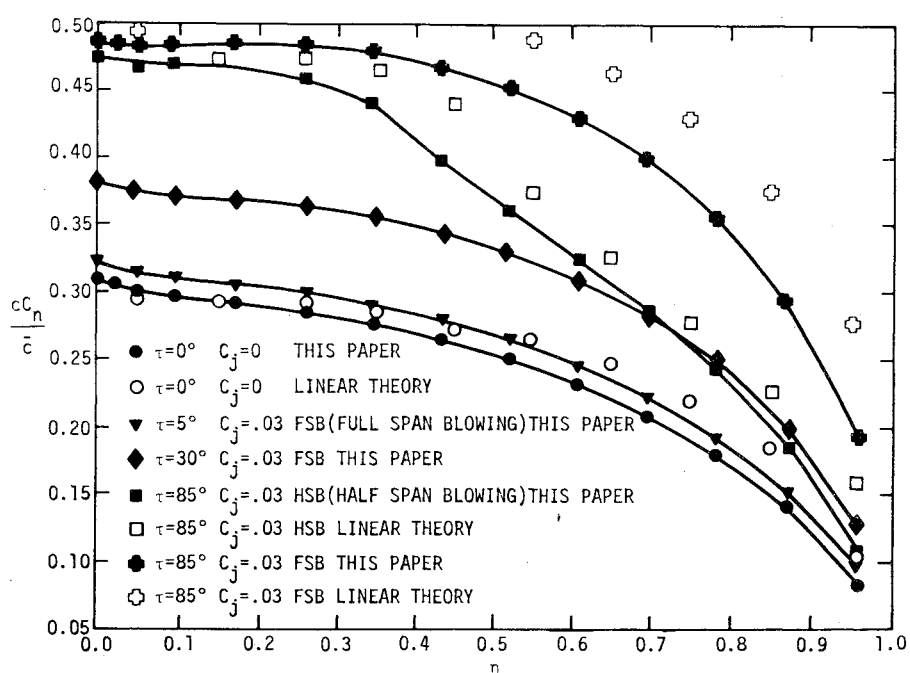


Fig. 5 Computed lift coefficient of jet-flapped ONERA M6 wing at various flap angles,  $\tau$ ,  $M_\infty = 0.84$ ,  $\alpha = 3^\circ$ ,  $C_j = 0.03$ ,  $\Lambda = 30^\circ$ ,  $\lambda = 0.538$ ,  $AR = 3.86$ .

and is presumably due to the limited extent of supercriticality in the flow, which is away from the trailing edge region.

In Fig. 7a, fine (68\*35\*36) grid results for chordwise pressures for the fully blown tapered ONERA M6 configuration for  $M_\infty = 0.84$ ,  $\alpha = 3^\circ$ ,  $\tau = 30^\circ$  and  $C_j = 0.03$  are compared with unblown results of Ref. 7 for the same wing. Considerable enhancement of the lifting pressures is indicated. The blown  $C_L$  is 0.424, as compared to an unblown value of 0.264. Blowing appears to move the shock downstream. This trend is consistent with the observations of Yoshihara<sup>13</sup> in which the shock can be moved aft of the trailing edge with sufficient blowing, thereby alleviating separation. It is also evident from the figure that such features as the increase in suction peaks at the tip would be totally inaccessible to recently proposed applications of sweepback and strip theories.

As a point of interest, the behavior of the pressure in the vicinity of the leading and trailing edges is shown in Fig. 7b. Singular character is quite evident near both locations as well

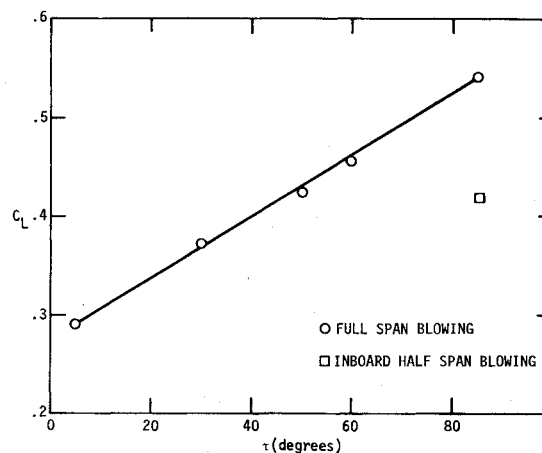


Fig. 6 Spanwise distribution of normal force—comparison of nonlinear and linear theories for ONERA M6 wing with jet flap.

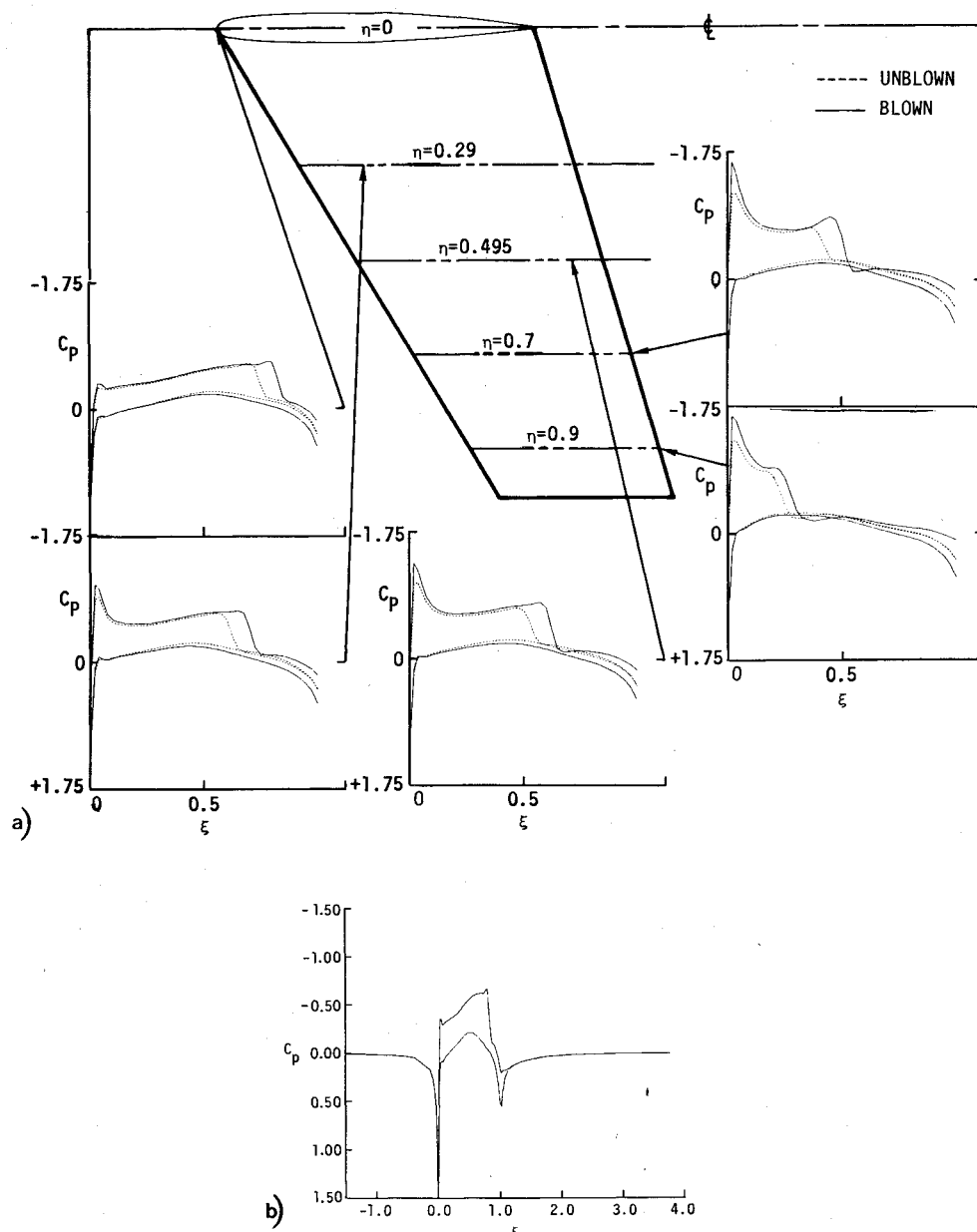


Fig. 7 a) Chordwise pressures on a jet-flapped, tapered wing,  $\Lambda = 30^\circ$ ,  $\lambda = 0.538$ ,  $AR = 3.86$ ,  $M_\infty = 0.84$ ,  $\alpha = 3^\circ$ ,  $C_j = 0.03$ , ONERA M6 section full span blowing. b) Root ( $\eta = 0$ ) chordwise pressures on tapered wing of Fig. 7a.

as a rapid decay of the vorticity downstream of the trailing edge. This behavior provides some basis for the differencing procedures previously described in which  $[\Phi_{\xi\xi}]$  is assumed to vanish in this region. However, a more thorough analysis of the discarding of the correct averaging procedures should be investigated in future research. Within the framework of this paper, these studies also should explore the effect of the transfer of the boundary conditions to the  $z=0$  plane, more accurate characterizations of the trailing edge singularity, the wake and jet spreading effects recently described in Ref. 14, and the relaxation of the boundary condition (4') for the first two  $\xi$  mesh points to the right of the jet exit. In spite of the approximations, the present theory when applied two dimensionally gives encouraging agreement with experiments. Additional data for three-dimensional configurations should be obtained to establish limitations in application of small disturbance theory for large jet deflection angles and appreciable viscous effects. No three-dimensional wing-alone supercritical jet flap pressure data were available at the time of publication for comparison with the present results.

Although we have applied the linearized boundary conditions (3-5) to the case of large jet deflection angles, where the small disturbance approximation is invalid, four other researchers have noted that agreement with either experiments or nonlinear jet-flap boundary conditions is excellent. Spence<sup>15</sup> obtains close agreement with the available experiments for deflection angles as large as  $60^\circ$  using an incompressible flow model applied to a flat plate. Halsey<sup>16</sup> developed a computer program also for incompressible flow using both linear and nonlinear jet-flap boundary conditions applied to wings as well as airfoils. He observes that "for cases with no flaps, moderate camber, and out-of-ground effect, linear theory is remarkably accurate" even with jet deflection angles as large as  $90^\circ$ .

For the case of transonic flow, Ives and Melnik<sup>1</sup> compare both linear and nonlinear jet-flap boundary conditions using the full compressible flow equations. They observe that for a deflection angle of  $30^\circ$  the pressure distribution is nearly the same for both boundary conditions, "indicating that the linearized jet-flap boundary condition is adequate for engineering purposes." Finally, in a revision of our earlier paper<sup>17</sup> using essentially the same basic algorithms of this paper but applied to airfoils, we obtain good agreement with experimental pressure data even at a jet deflection angle of  $85^\circ$ .

### Conclusions

An algorithm has been developed which treats transonic flow over jet-flapped wings within a small disturbance framework. The numerical method employs a far-field asymptotic representation which is similar to that of incompressible lifting line theory with an added bound vorticity contribution along the span due to the jet. Computational results for a variety of planforms give rise to the following additional observations.

1) Chordwise pressures at various span stations indicate repeal of the Kutta condition in the same manner as that observed for supercritical two-dimensional airfoils.

2) For configurations in which only a portion of the span is active (partial span blowing), there is an appreciable carryover of the lift augmentation from the blown to unblown sections. This confirms experimental observations of Yoshihara and his co-workers.

3) For moderately supercritical planforms with blunt-nosed symmetric sections, the jet flap augmentations in lift,

moment, and normalized spanwise loadings are qualitatively similar to those predicted by linearized lifting surface methods. This statement is particularly correct for limited supercriticality away from the trailing edge. Nevertheless, the anticipated significant discrepancies in chordwise loadings and drag due to shocks and nonlinearities also are evident.

4) Terminating shocks for the supersonic region can be moved rearward and presumably downstream of the trailing edge by sufficient blowing, in agreement with experimental evidence of Yoshihara et al.

5) In agreement with data and incompressible behavior, the calculations demonstrate that for all other factors remaining the same, the lift augmentation due to blowing is reduced by sweepback.

### References

- Ives, D.C. and Melnik, R.E., "Numerical Calculation of the Compressible Flow Over an Airfoil with a Jet Flap," AIAA Paper 74-542, Palo Alto, Calif., 1974.
- Malmuth, N.D. and Murphy, W.D., "A Relaxation Solution for Transonic Flow Over Jet-Flapped Airfoils," AIAA Paper 75-82, Pasadena, Calif., 1975.
- Klunker, E.B., "Contribution to Methods for Calculating the Flow About Thin Lifting Wings at Transonic Speeds—Analytical Expressions for the Far Field," NASA TND-6530, Nov. 1971.
- Murman, E.M. and Cole, J.D., "Calculation of Plane Steady Transonic Flows," *AIAA Journal*, Vol. 9, Jan. 1971, pp. 114-121.
- Krupp, J.A. and Murman, E.M., "Computation of Transonic Flows Past Lifting Airfoils and Slender Bodies," *AIAA Journal*, Vol. 10, July 1972, pp. 880-886.
- Ballhaus, W.F. and Bailey, F.R., "Numerical Calculation of Transonic Flow About Swept Wings," AIAA Paper 72-677, Boston, Mass., 1972.
- Bailey, F.R. and Ballhaus, W.F., "Comparisons of Computed and Experimental Pressures for Transonic Flows About Isolated Wings and Wing-Fuselage Configurations," *Proceedings of the Conference on Aerodynamic Analyses Requiring Advanced Computers, Part II*, NASA SP-347, 1975, pp. 1213-1232.
- Van Dyke, M., *Perturbation Methods in Fluid Mechanics*, Academic Press, New York, 1964, pp. 167-176.
- Murman, E.M., "Analysis of Embedded Shock Waves Calculated by Relaxation Methods," *Proceedings of the Computational Fluid Dynamics Conference*, July 19-20, 1973, Palm Springs, Calif., pp. 27-40.
- Poisson-Quinton, Ph. and Jousserandot, P., "Influence du Soufflage au Voisinage du Bord de Fuite sur les Caracteristiques Aerodynamiques d'une Aile aux Grandes Vitesses," *La Recherche Aeronautique*, No. 56, Feb. 1957, pp. 21-32.
- Poisson-Quinton, Ph. and LePage, L., "Survey of French Research on the Control of Boundary Layer and Circulation," *Boundary Layer and Flow Control*, Vol. 1, Pergamon Press, London, 1961, pp. 21-73.
- Malavard, L., "Application of the Rheoelectric Analogy for the Jet Flap Wing of Finite Span," *Boundary Layer and Flow Control*, Vol. 1, Pergamon Press, London, 1961, pp. 365-389.
- Yoshihara, H., Benepe, D., and Whidden, P., "Transonic Performance of Jet-Flaps on Advanced Fighter Configuration," Air Force Flight Dynamics Lab., Wright-Patterson AFB, Ohio, AFFDL-TR-73-97, 1973.
- Yoshihara, H. and Zonars, D., "The Transonic Jet Flap—A Review of Recent Results," *National Aerospace Engineering and Manufacturing Meeting*, Culver City, Calif., Paper 751089, Nov. 17-20, 1975, Culver City, Calif.
- Spence, D.A., "The Lift Coefficient of a Thin Jet-Flapped Wing," *Proceedings of the Royal Society (London)*, Vol. A238, Dec. 1956, pp. 46-68.
- Halsey, N.D., "Methods for the Design and Analysis of Jet-Flapped Airfoils," AIAA Paper 74-188, Washington, D.C., 1974.
- Malmuth, N.D. and Murphy, W.D., "A Relaxation Solution for Transonic Flow Over Jet Flapped Airfoils," *AIAA Journal*, Vol. 14, Sept. 1976, pp. 1250-1257.